Multiphase Coupled-Buck Converter—A Novel High Efficient 12 V Voltage Regulator Module

Peng Xu, *Member, IEEE*, Jia Wei, and Fred C. Lee, *Fellow, IEEE*

***Abstract*—The most popular VRM topology—multiphase buck converter operates at a very small duty cycle due to a high input voltage and a low output voltage. The performance of the multiphase buck converter suffers from the very small duty cycle. Alternative topologies with an extended duty cycle are explored in order to improve the efficiency without compromising the transient response. A novel topology named multiphase coupled-buck converter is proposed, which enables the use of a large duty cycle with recovered leakage energy and clamped MOSFET voltage. The input filter is further integrated in the proposed circuit to reduce the number of components. A 12 V-to-1.5 V/50 A VRM prototype demonstrates that the multiphase coupled buck converter can have a much better efficiency than the multiphase buck converter with the same transient response.**

***Index Terms*—Active clamping circuit, built-in filter, coupled inductors, multiphase converter, voltage regulator module.**

I. Introduction

ADVANCES in VLSI technologies impose challenges in the design of power supplies for microprocessors [1]. In order to deliver a highly accurate supply voltage to microprocessors, a dedicated dc/dc converter, so-called voltage regulator module (VRM) is placed in close proximity to the microprocessors. Most of today's VRM topologies are based on the multiphase buck converter [2]–[5].

In the multiphase buck converter, the duty cycle is the ratio of the output voltage and input voltage. The earlier VRMs use 5 V as the input, where the synchronous buck topology works very well. The latest microprocessors for desktop computers, workstations, and low-end servers, require VRMs to work with 12 V input. In laptop computers, VRMs directly step from the battery charger voltage of 16–24 V down to the microprocessor voltage. Meanwhile, the microprocessor voltage is expected to decrease to below 1 V [1]. For these applications, the multiphase buck converter is required to operate at a very small duty cycle.

The influence of duty cycle on the performance of the multiphase buck converter is investigated in this paper. With a very small duty cycle, the benefit of multiphase buck converter as far as using a small inductance to improve the transient response is compromised due to the poor ripple cancellation. The efficiency of the multiphase buck converter also suffers from a very small duty cycle, mainly due to the increased switching loss in the control MOSFETs.

Alternative topologies [6]–[9] with an extended duty cycle are explored in order to improve the efficiency without compromising the transient response. The multiphase tapped-inductor buck converter is one of the simplest topologies with an extended duty cycle. Multi-winding coupled inductors are used to enlarge the duty cycle. However the leakage inductance between coupled inductor windings causes severe voltage spikes across MOSFETs.

This paper proposes an improved topology named the multiphase coupled-buck converter, which uses the existing coupled inductor windings to form an active clamping circuit between interleaved channels to solve the voltage spike problem. The proposed topology enables the use of a large duty cycle with recovered leakage energy and clamped MOSFET voltages. Both analysis and experiment show that the multiphase coupled-buck converter can achieve a much better efficiency than the multiphase buck converter with the same transient response.

The input filter is further integrated in the proposed topology to reduce the number of components. Compared to the original multiphase coupled-buck converter, the improved multiphase coupled-buck converter has smoother input and output currents.

II. Limitations of Multiphase Buck Converter

Fig. 1 shows the multiphase buck converter, which is the most common of today's VRM topologies.

A. Influence of Duty Cycle on Ripple Cancellation

One of the major advantages of the multiphase buck converter is the ripple cancellation effect, which enables the use of a small inductance to improve the transient response and to minimize the output capacitance.

In the multiphase buck converter, the inductor current ripples in individual channels are cancelled at the output and the total ripple current flowing into the output capacitors is reduced. With such ripple cancellation, the output voltage ripple becomes very small, which allows more room for voltage deviations during load transients. A small inductance can be used to improve the transient response, and consequently a small output capacitance can be used to meet the transient requirements.

For the multiphase buck converter, the magnitude of the output current ripples can be derived as

$$\Delta I_L = \frac{V_o(1-D)}{LoF_s}\,\frac{N\left(D-\frac{m}{N}\right)\left(\frac{m+1}{N}-D\right)}{D(1-D)} \qquad (1)$$

Manuscript received April 11, 2001; revised September 19, 2002. This work was supported by Delta Electronics, Hipro, Hitachi, Intel, Intersil, National Semiconductors, Power-One, TDK, Texas Instruments, and the ERC Program of the National Science Foundation under Award EEC-9731677. Recommended by Associate Editor N. Femia.

P. Xu is with Philips Research, Briarcliff Manor, NY 10510 USA (e-mail: peng.xu@philips.com).

J. Wei and F. C. Lee are with the Center for Power Electronics Systems, the Bradley Department of Electrical and Computer Engineering, Virginia Polytechnic Institute and State University, Blacksburg, VA 24061 USA.

Digital Object Identifier 10.1109/TPEL.2002.807082

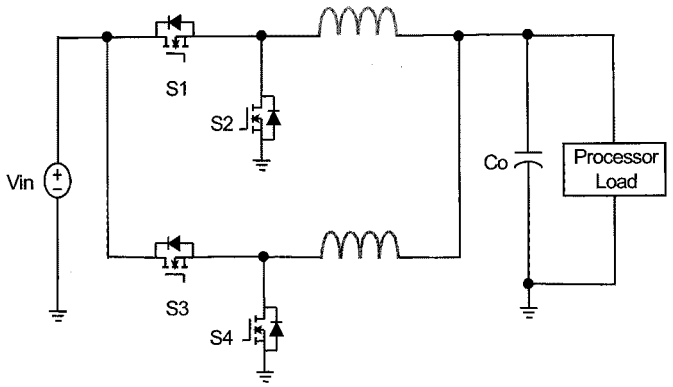

Fig. 1. Multiphase buck converter for VRM applications.

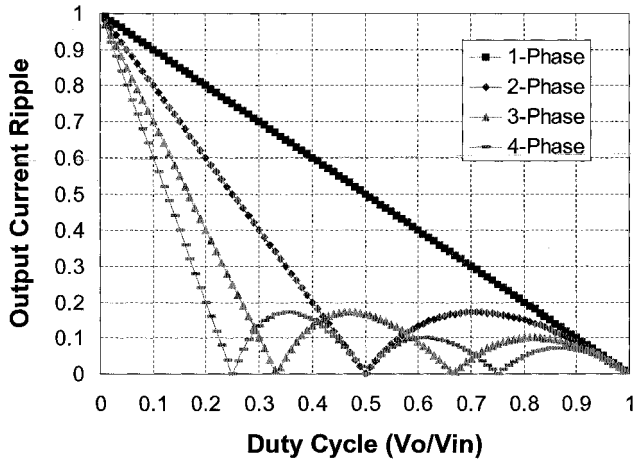

Fig. 2. Influence of duty cycle on current ripple cancellation.

where N, Lo and Fs are the channel number, the output inductance per channel and the switching frequency, respectively. $m = floor(N \cdot D)$ is the maximum integer that does not exceed the $N \cdot D$.

Fig. 2 plots the influence of duty cycle on the output current ripple. The output current ripple is normalized against the inductor current ripple at zero duty cycle.

As can be seen from Fig. 2, with a very small duty cycle, the current ripple cancellation is poor in the multiphase buck converter. Thus the benefit of the multiphase buck converter as far as using a small inductance to improve the transient response is compromised.

B. Influence of Duty Cycle on Efficiency

In the multiphase buck converter, a small duty cycle causes large current ripples in the inductors, which increase the conduction and switching losses of MOSFETs, as well as the losses in the inductors.

Fig. 3 shows the measured efficiencies for a tested four-phase synchronous buck VRM with two different input voltages, 5 V and 12 V. The output voltage, output current and switching frequency are 1.5 V, 50 A, and 300 kHz, respectively. The measured efficiency data include the power losses in the power stage, but exclude the control and gate drive losses. Fig. 4

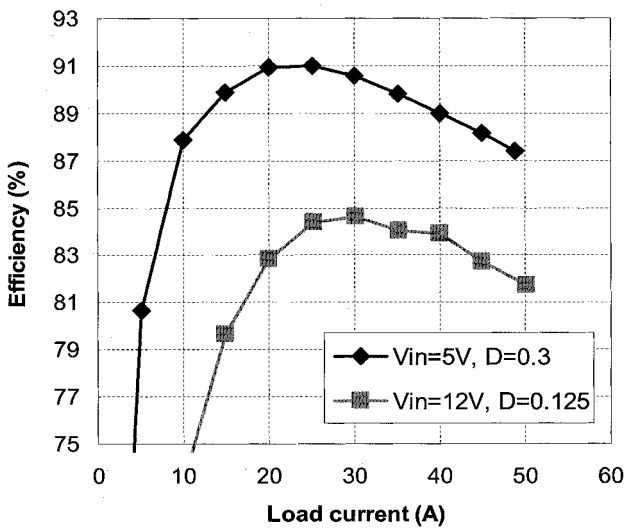

Fig. 3. Measured efficiency of four-phase buck VRM with $V_{IN} = 5$ V and 12 V.

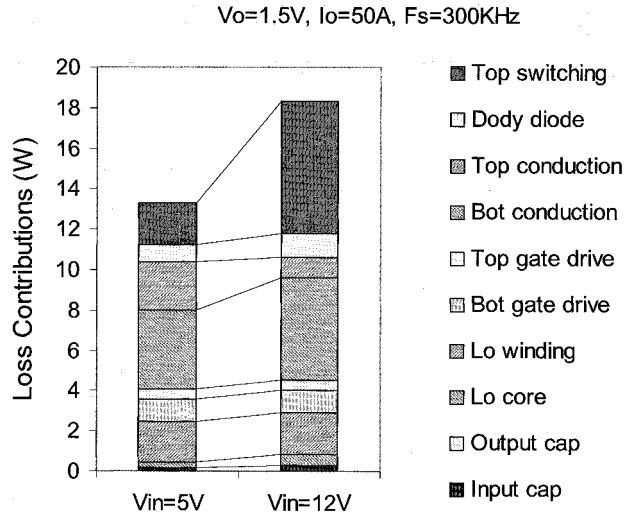

Fig. 4. Loss contributions in four-phase buck VRM with $V_{IN} = 5$ V and 12 V.

shows the estimated loss contributions at full load for the tested VRM.

As can be seen from Fig. 4, the 5 V input VRM can achieve 87% efficiency at full load and 91% peak efficiency, while the 12 V input VRM can only reach 81% efficiency at full load and 84.5% peak efficiency. With the increase of input voltage from 5 V to 12 V, the duty cycle is decreased from about 0.3 to 0.125. The decrease of the duty cycle reduces the full-load efficiency by about 6% and peak efficiency by about 7%. This efficiency drop is mainly caused by the increased switching loss in the control MOSFETs, as can be seen from the loss contributions shown in Fig. 4. The switching loss in the control MOSFETs is increased by about 5 W, which causes more than 5% efficiency drop at full load.

In summary the efficiency of the multiphase buck converter suffers from a very small duty cycle, mainly due to the increased switching loss in the control MOSFETs.

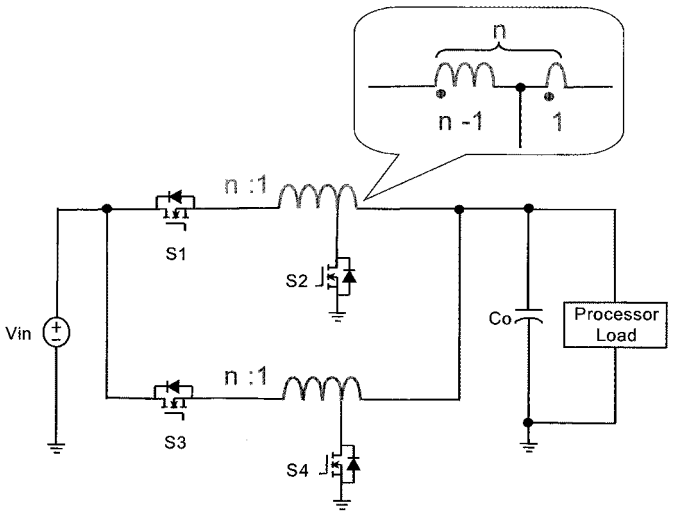

Fig. 5. Multiphase tapped-inductor buck converter.

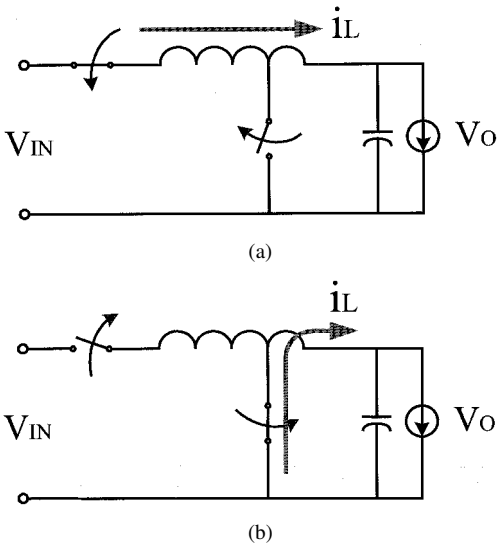

Fig. 6. Equivalent circuits of tapped-inductor buck converter during: (a) step up transient and (b) step down transient.

III. Multiphase Tapped-Inductor Buck Converter

Several methods exist for extending the duty cycle of the buck converter [6]–[9]. Among them, the tapped-inductor buck converter is one of the simplest topologies with an extended duty cycle. The biggest advantage of the tapped-inductor buck converter over other proposed solutions is the fact that it only involves a slight modification of the original buck converter.

Fig. 5 shows multiphase tapped-inductor buck converter. The turns ratio of the tapped inductor is defined as the turns number of the winding in series with the control MOSFET over that of the winding in series with the synchronous MOSFET.

A. Extended Duty Cycle

In the multiphase tapped-inductor buck converter, the DC voltage gain is a function of both the duty cycle D and the turns ratio n, which can be derived as

$$\frac{V_o}{V_{IN}} = \frac{D}{D + n \cdot (1 - D)}. \tag{2}$$

As can be seen from Equation (2), the higher the turns ratio, the larger the resulting duty cycle will be. For the multiphase tapped-inductor buck converter, the desirable turns ratio is related to the transient response.

The duty cycle is assumed to become "saturated" during transients to achieve a fast transient response. That is, the duty cycle $D = 1$ for step-up transient, and the duty cycle $D = 0$ for step-down transient. Fig. 6 shows the equivalent circuits of tapped-inductor buck converter during step-up and step-down transients. During a step-up transient, the top switch is on and the bottom switch is off. During a step-down transient, the bottom switch is on and the top switch is off.

The difference between the load current and the inductor current causes the unbalanced charge that must be provided by the output capacitors. The higher the inductor slew rate during transients, the smaller the unbalanced charge area will be, and the better the transient response thus can be obtained. Fig. 7 shows the inductor slew rates during both the step-up and step-down transients as a function of the turns ratio. Although it is desirable

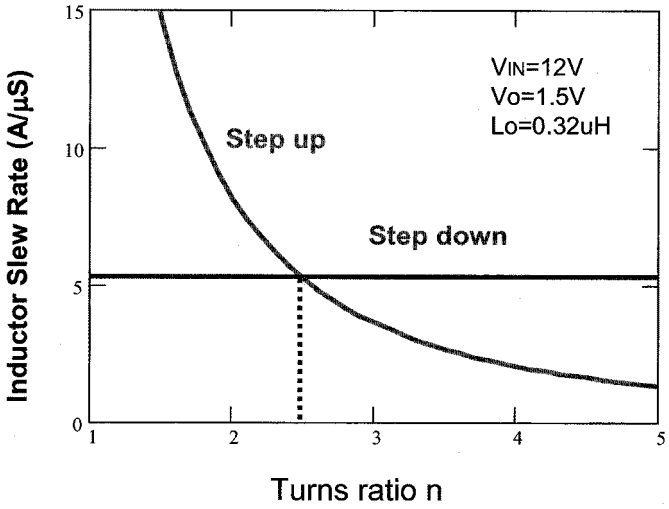

Fig. 7. Inductor slew rates during transients for tapped-inductor buck converter.

to choose a high turns ratio to obtain a large duty cycle, a high turns ratio, at which the inductor slew rate of the step-up transient is lower than that of the step-down transient, will impair the overall transient performance. The desirable turns ratio is chosen to achieve the same transient inductor slew rates for both step-up and step-down transients. For a VRM stepping down from 12 V to 1.5 V, the desirable turns ratio is 2 : 1. The multiphase tapped-inductor buck converter operates at 0.225 duty cycle, while the duty cycle of multiphase buck converter is only 0.125.

B. Voltage Spike Problem

In the multiphase tapped-inductor converter, leakage inductance existing between two coupled windings causes a voltage spike across MOSFETs. The leakage energy is also dissipated and generates great power losses.

Fig. 8 shows the measured switching waveforms in the tested four-phase tapped-inductor buck VRM. A huge voltage spike is observed across the control MOSFET. The spike voltage is

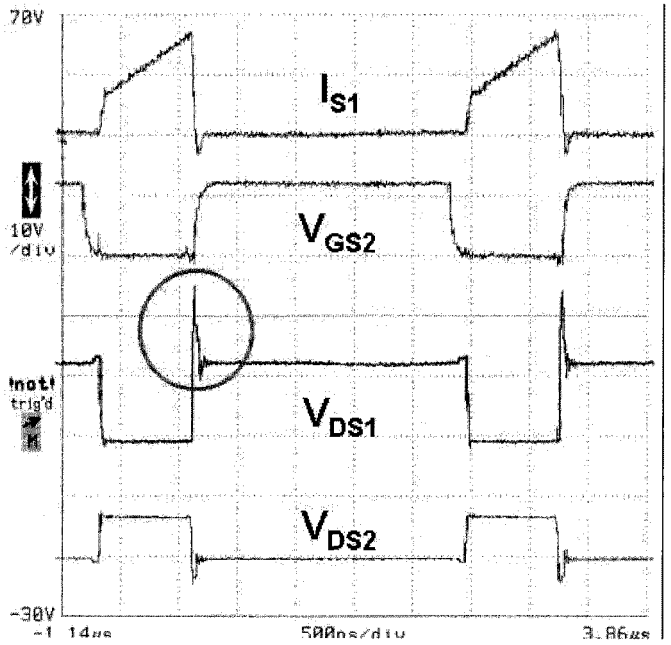

Fig. 8. Measured switching waveform shows a huge voltage spike across control MOSFET.

higher than 30 V and causes the failure of the MOSFET that typically has no more than 30 V breakdown voltage. The huge voltage spike is caused by the resonance between the leakage inductance and the output capacitance of MOSFETs when the control switch turns off.

Clamping or snubber circuits have to be used to solve the voltage spike problem. However, these require many additional components. For multiphase topologies, this solution would impose significant increases in both the cost and complexity of the circuit.

IV. Multiphase Coupled-Buck Converter

In order to solve the voltage spike problem of the multiphase tapped-inductor buck converter, an improved topology named multiphase coupled-buck converter is proposed, which uses the existing coupled inductor windings to form an active clamping circuit between interleaved channels.

A. Concept of Multiphase Coupled-Buck Converter

The idea is derived from the multiphase tapped-inductor buck converter with an active clamping circuit for each channel in order to solve the voltage spike problem, as shown in Fig. 9.

Each channel has an active clamping circuit formed by a capacitor and a MOSFET. The capacitor has a constant voltage in steady-state operation, which serves as a voltage source. The MOSFETs S1a and S2a have the same control timings as bottom switches S2 and S4, respectively. After top switch S1 or S3 turns off, the current trapped in the leakage inductance forces the body diode of S1a or S2a to conduct. Consequently, the drain–source voltage of top switch S1 or S3 is clamped to the input voltage plus the clamping capacitor voltage, and the leakage energy is

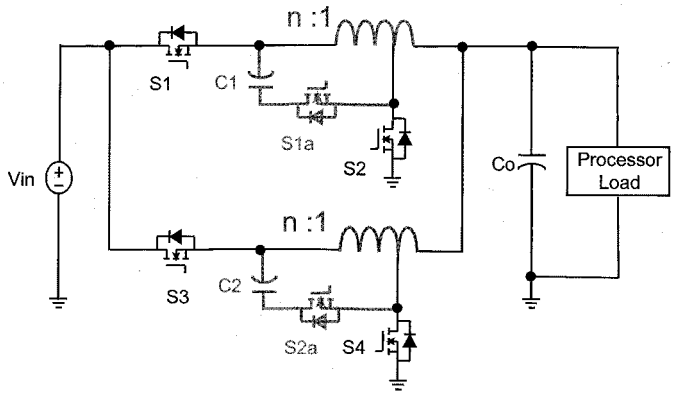

Fig. 9. Multiphase tapped-inductor buck converter with an additional active clamping circuit for each channel.

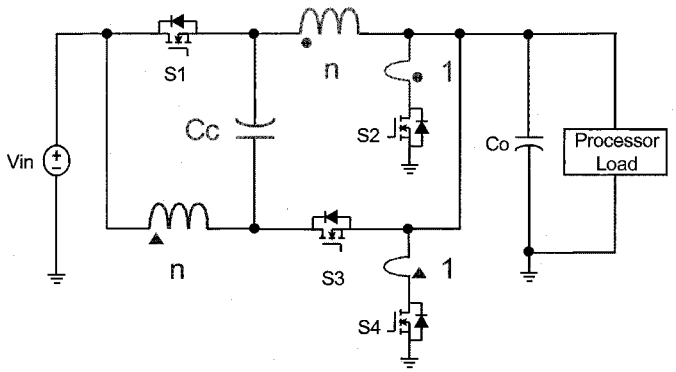

Fig. 10. Active clamping circuits formed between neighbor channels with a variable capacitor voltage.

stored in the clamping capacitors C1 or C2 and is recovered to the load later.

Since multiphase topologies already have many switches, the idea is that neighboring channels can probably be rearranged so that the existing switches can incorporate the function of the additional switches S1a and S2a. Fig. 10 shows a resulting configuration. The topology is very simple. Top switches S1 and S2 have two functions: they serve as the control switches for their own channels and meanwhile, also serve as the active clamping switches for neighbor channels. In order to realize this active clamping concept, the capacitor Cc has to appear as a constant voltage, as shown in Fig. 10. However, further investigation finds that this capacitor does not have a constant voltage. The reasons are that switches S1 and S3 do not switch complementarily, and the two top windings in the neighbor channels have different voltages across them.

A modification is made in order to allow the clamping capacitor to have a constant voltage. The resulting topology, called the multiphase coupled-buck converter, is shown in Fig. 11. As shown in Fig. 11, a third winding is coupled with the output inductor of the neighbor channel and is placed in series with the existing top winding. The voltage induced in the third winding compensates the voltage of the existing top winding in the neighbor channel, and therefore, the clamping capacitor appears as a constant voltage, which equals the input voltage minus output voltage.

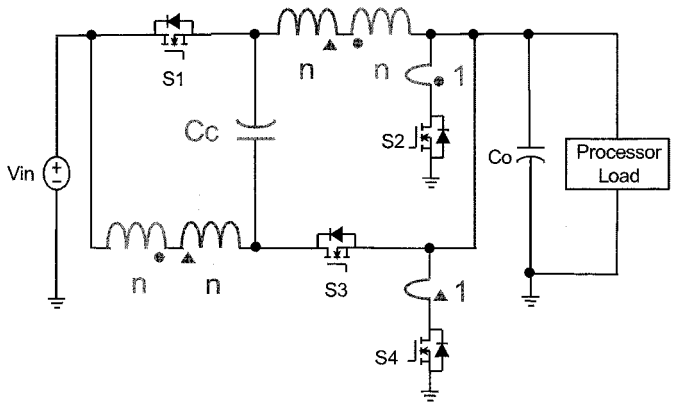

Fig. 11. Proposed multiphase coupled buck converter.

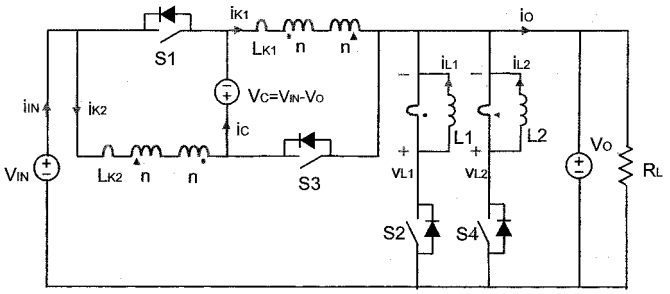

Fig. 12. Simplified multiphase coupled-buck converter for steady-state analysis.

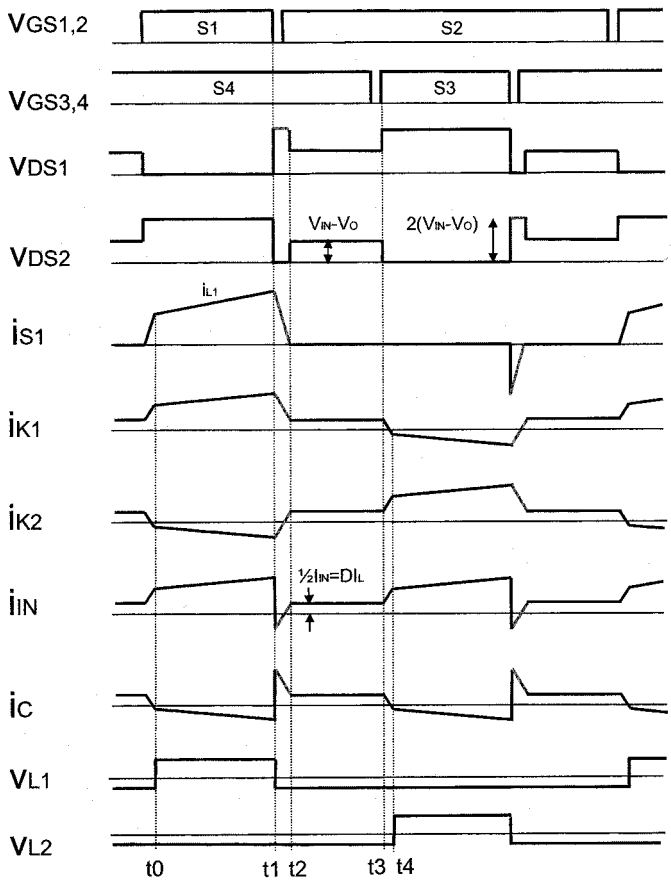

Fig. 13. Key operation waveforms of multiphase coupled-buck converter.

B. Steady-State Operation

Fig. 12 shows the simplified circuit for steady-state analysis. The clamping capacitor is assumed to be large enough and is treated as a voltage source. The coupled output inductors have three windings, and are modeled as a three-winding transformer paralleled with a discrete inductor. All the semiconductor devices are treated as ideal switches.

Fig. 13 shows the key operation waveforms. Fig. 14 shows the equivalent circuits for the different stages. The operation during these stages can be briefly described as follows.

Stage I (t0–t1) corresponds to the buck mode. As shown in Fig. 14(a), S1 is on, S2 is off, S3 is off, and S4 is on. The input source and the clamping capacitor feed energy to the output through output inductor L1. Inductor L2 is freewheeling. The stage ends when the control signals turn S1 off and S2 on.

Stage II (t1–t2) corresponds to the leakage energy recovery mode. As shown in Fig. 14(b), S1 is off, S2 is on, the body diode of S3 is on, and S4 is on. The drain–source voltage of S1 is clamped to the sum of the clamping voltage and the input voltage. The leakage energy is recovered to the clamping capacitors. Inductors L1 and L2 are both freewheeling. The stage ends when the body diode of S3 turns off.

Stage III (t2–t3) corresponds to the freewheeling mode. As shown in Fig. 14(c), S1 is off, S2 is on, S3 is off, and S4 is on. Inductors L1 and L2 are both freewheeling. The input voltage feeds energy to the clamping capacitor in order to maintain the balance of the charge in the clamping capacitor. The stage ends when a control turns S3 on.

Stage IV (t3–t4) corresponds to the leakage current reset mode. As shown in Fig. 14(d), S1 is off, S2 is on, S3 is on, and S4 is on. Inductors L1 and L2 are both freewheeling. The S3 current increases. The stage ends when the S3 current reaches the level of the output inductor current. Then, stage I begins again.

As can be seen from Fig. 13, the proposed multiphase coupled-buck converter is immune to the leakage inductance. The drain–source voltages of the top switches are clamped to two times the input voltage minus output voltage. For a VRM stepping down from 12 V to 1.5 V, the voltage stress for top switches is 21 V and therefore typical 30 V MOSFETs can be used with a sufficient safety margin.

According to the steady-state operation waveforms, the DC voltage gain of the multiphase coupled-buck converter can be derived as

$$\frac{V_o}{V_{IN}} = \frac{D}{D+n}. \tag{3}$$

Following the same discussion on the selection of the turns ratio as in Section III, the desirable turns ratio is chosen for multiphase coupled-buck converter to achieve the same transient inductor slew rates for both step-up and step-down transients. For a VRM stepping from 12 V to 1.5 V, the desirable turns ratio is 2 : 1. The multiphase coupled-buck converter operates at 0.286 duty cycle, while the duty cycle of multiphase buck converter is only 0.125.

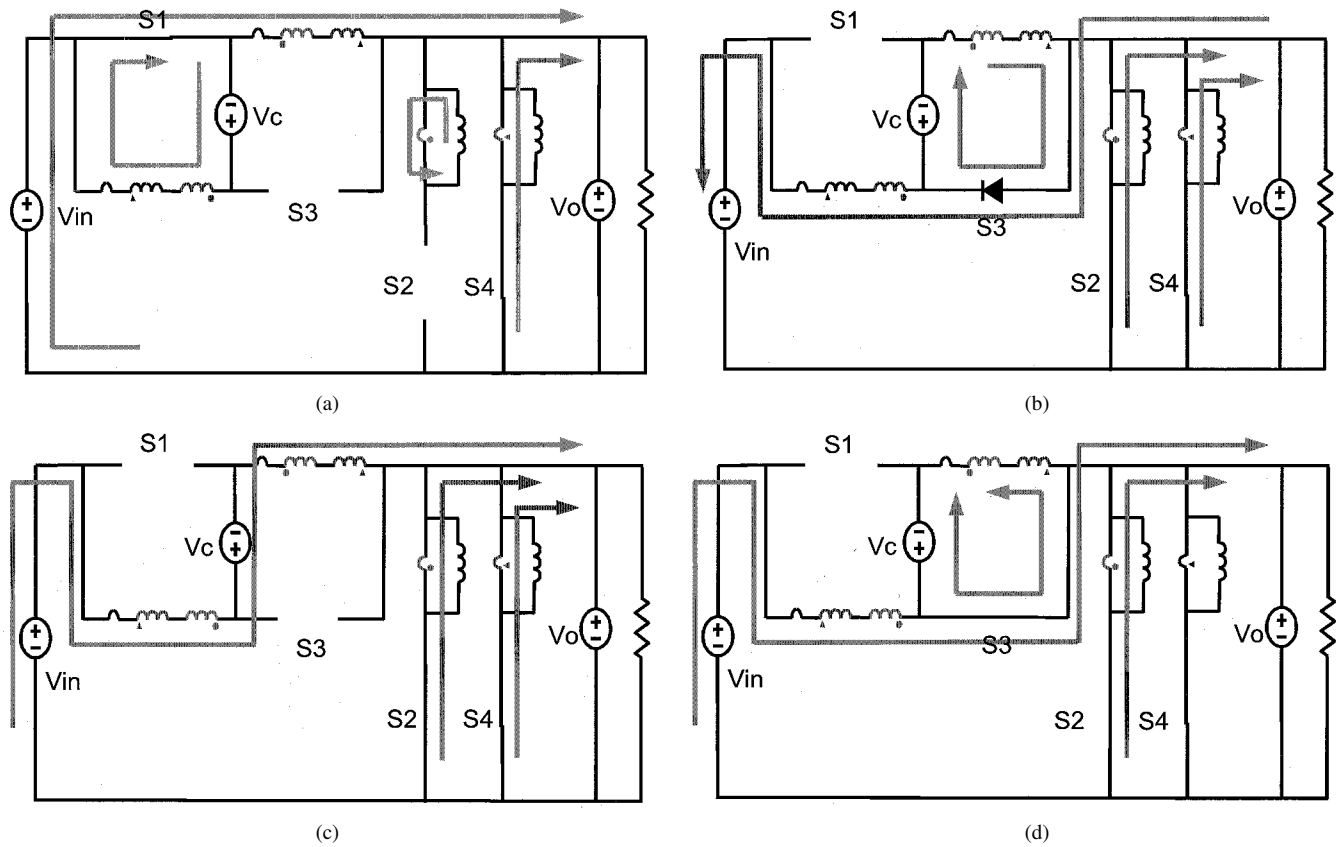

Fig. 14. Equivalent circuits of multiphase coupled-buck converter: (a) Stage I, (b) Stage II, (c) Stage III, and (d) Stage IV.

C. Small Signal Modeling

To study the dynamic performance of multiphase coupled-buck converter, an average model was developed and verified experimentally [10]. Here, the control-to-output transfer function is taken for the following discussion. For a two-phase coupled-buck converter, it can be derived as

$$G_{vd}(s) = V_{IN}\frac{n}{(D+n)^2}\cdot\frac{\left(1+\frac{s}{z_1}\right)\left(1+\frac{s}{z_2}\right)}{\left(1+\frac{s}{\omega_0 Q}+\left(\frac{s}{\omega_0}\right)^2\right)\left(1+\frac{s}{\omega_1}\right)} \tag{4}$$

where

$$z_1 = -\frac{1}{RcCo},\quad z_2 = -\frac{2(D+n)^2 Rc}{DnLo},\quad \omega_1 = -\frac{1}{RcCc},$$
$$\omega_0 = \frac{D+n}{n}\sqrt{\frac{2}{LoCo}},\ \text{and}\ Q = \frac{n}{D+n}\cdot\frac{1}{R_1}\cdot\sqrt{\frac{Lo}{2Co}}.$$

Lo is the output inductance reflected to the winding in series with the synchronous MOSFET, Cc is the clamping capacitance, Co is the output capacitance, and Rc is the equivalent series resistance (ESR) of the output capacitor.

As can be seen from (4), there are three poles and two zeros. One pole comes from the clamping capacitor and the ESR of the output capacitor. In practice, this is a very high-frequency pole in the order of tens of MHz so that it does not affect the frequency range of loop-gain bandwidth. There is also a double pole. This double pole moves as a function of the output inductance, the output capacitance and the duty cycle, but not as a function of the load. Of the two zeros, one is the ESR zero introduced by the output capacitor, and the other is an interesting left-half-plane (LHP) zero. Unlike the right-half-plane (RHP) zero of the tapped-inductor buck converter reducing loop-gain bandwidth [7] and consequently slowing the transient response, this LHP zero is good for loop-gain design since it can provide an additional phase margin without reducing loop-gain bandwidth. Thus, the multiphase coupled-buck converter is suitable to achieve a wide loop-gain bandwidth and consequently a fast transient response.

V. Improved Multiphase Coupled-Buck Converter With Built-In Filters

Since coupled inductors are used, the output current of the multiphase coupled-buck converter is pulsing. The pulsing output current increases the output ripple voltage and generates the switching noise across the equivalent series inductor (ESL) and ESR of the output capacitors. Additional L–C filters are used to smooth the pulsing currents as shown in Fig. 15.

This paper further proposes an improved multiphase coupled-buck converter with built-in filters. As shown in Fig. 16, the improved multiphase coupled-buck converter has smooth input and output currents without additional L–C filters. The existence of built-in filters reduces the number or size of filter components.

The integration of built-in input and output filters is explained in Fig. 17. Starting from the original multiphase coupled-buck converter with additional L–C filters, as shown in Fig. 15, and by using the shifting principle for capacitors, the filtering and

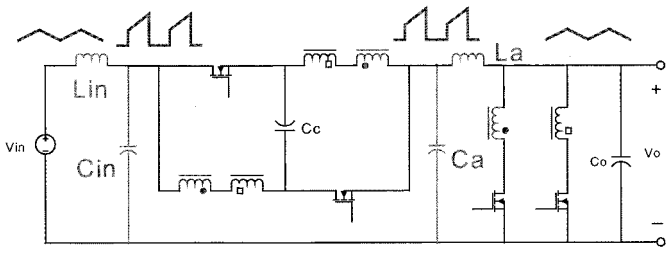

Fig. 15. Multiphase coupled-buck converter with additional L–C filters.

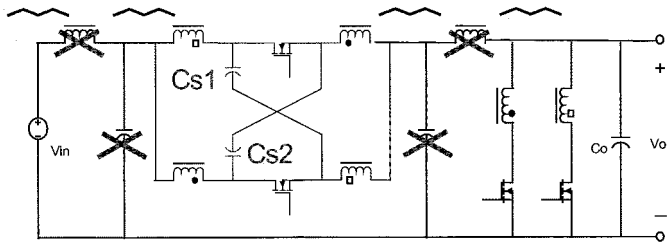

Fig. 16. Improved multiphase coupled-buck converter with built-in filters.

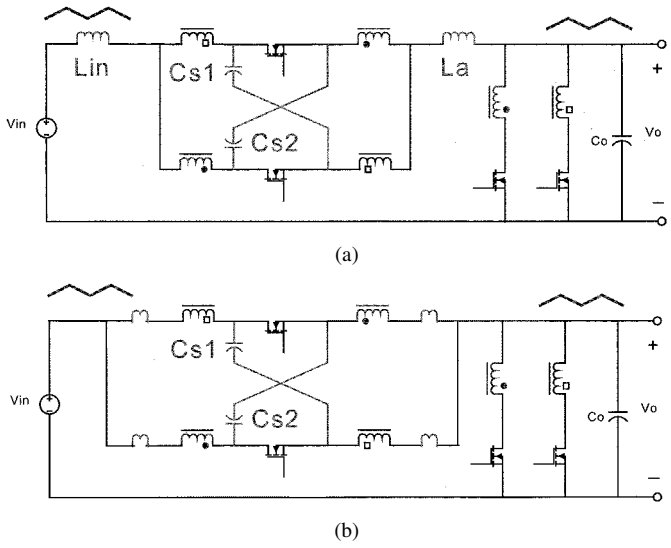

Fig. 17. Integration of L–C filters in multiphase coupled buck converter: (a) capacitor shifting and (b) inductor shifting.

clamping capacitors Cin, Ca and Cc can be shifted to new locations without changing the filtering and clamping functions, as shown in Fig. 17(a). Next by using the shifting principle for inductors, the filtering inductors Lin and La are shifted to the positions in series with the inductor windings without changing the basic operation of converter, as shown in Fig. 17(b). The resulting topology is an improved multiphase coupled-buck converter, where the leakage inductances of coupled windings are drawn.

Based on the preceding manipulations in the improved multiphase coupled-buck converter, the built-in filters are formed between the leakage inductance and the clamping capacitors C_{S1} and C_{S2}. This concept is similar to one used for other earlier applications [11]–[13].

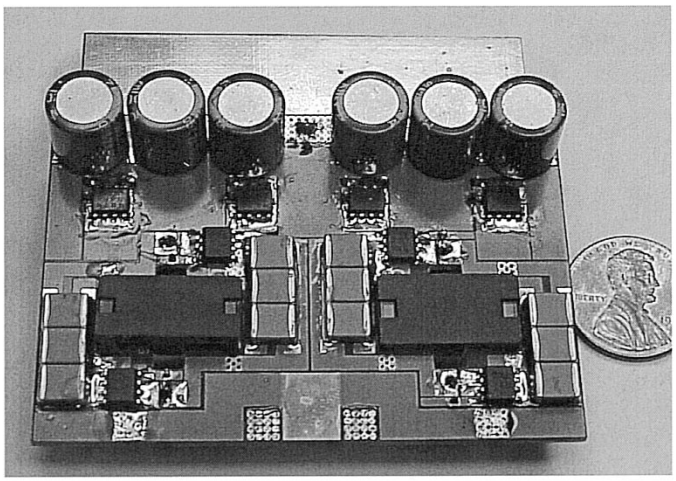

Fig. 18. 12 V VRM prototype using four-phase coupled buck converter with built-in filters.

VI. Experimental Results

12 V-input, 1.5 V/50A-output VRM prototypes were built using the improved four-phase coupled-buck converter. These prototypes, as shown in Fig. 18, operate at 300 kHz. The following components were selected for the power stage: control MOSFETs—Si4884DY; synchronous MOSFETs—Si4874DY; output inductance reflected to the windings in series with synchronous MOSFETs—300 nH; input capacitors—12 $\times$ 22 uF ceramic, and output capacitors—6 $\times$ 820 uF OSCON.

In order to evaluate the efficiency of the proposed multiphase coupled-buck converter, a four-phase buck VRM was also built. For a fair comparison, the four-phase coupled buck VRM is designed with the same MOSFETs, input capacitors and output capacitors, and operates at the same conditions as the four-phase buck VRM.

To make the efficiency comparison meaningful, the design of inductors is based on the same transients. Fig. 19 shows the transient responses of the four-phase coupled-buck VRM and the four-phase buck VRM. The two VRMs have almost the same transient waveforms as intended.

Fig. 20 shows the measured efficiency of the four-phase coupled-buck VRM and the four-phase buck VRM. The efficiency data include the power losses in the power stage, but exclude the control and gate drive losses. For the four-phase coupled buck-VRM, the full-load efficiency is more than 85%, and the peak efficiency is 89%. Compared to the four-phase buck VRM, the four-phase coupled buck VRM has an efficiency improvement of about 3.5% at full load and 4.5% peak efficiency.

To illustrate this efficiency improvement, the loss contributions are estimated for both experimental VRMs. Fig. 21 shows the loss contributions at full load for the four-phase coupled buck VRM and the four-phase buck VRM. The main difference comes from the switching loss of control MOSFETs and the conduction loss of synchronous MOSFETs. The four-phase coupled buck VRM has 1 W more conduction loss from synchronous MOSFETs than the four-phase buck VRM, but 5 W less switching loss from control MOSFETs. Compared to

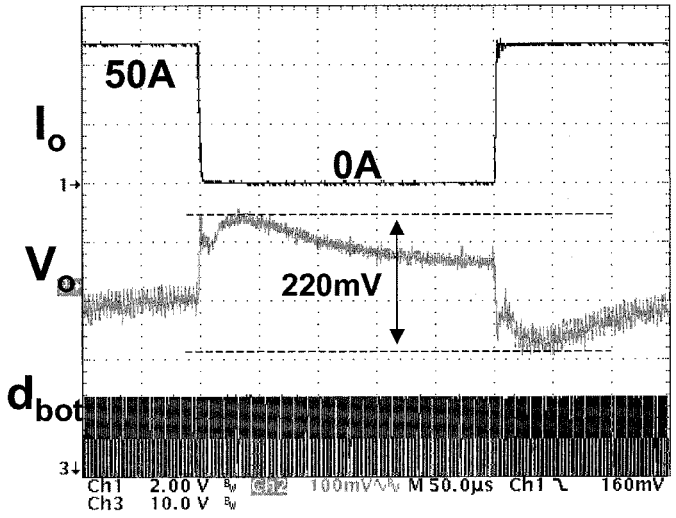

(a)

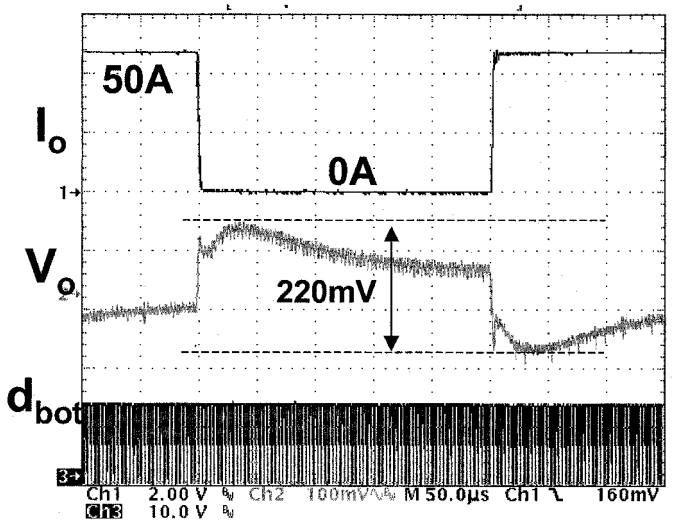

(b)

Fig. 19. Transient responses of: (a) four-phase coupled buck VRM and (b) four-phase buck VRM.

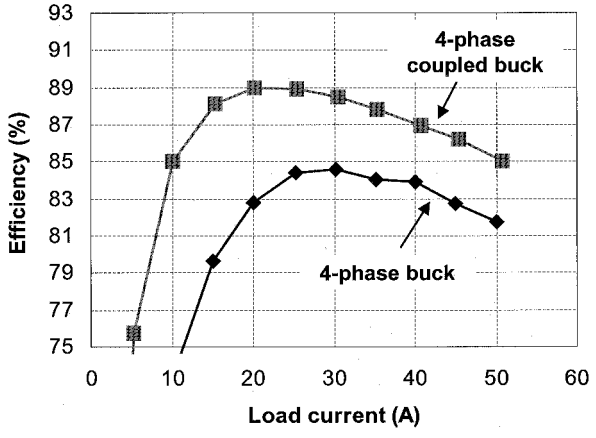

Fig. 20. Efficiency comparison between a four-phase coupled buck VRM and a four-phase buck VRM.

the four-phase buck VRM, the overall loss reduction for the four-phase coupled buck VRM is 4 W, which corresponds to 4% efficiency improvement at full load.

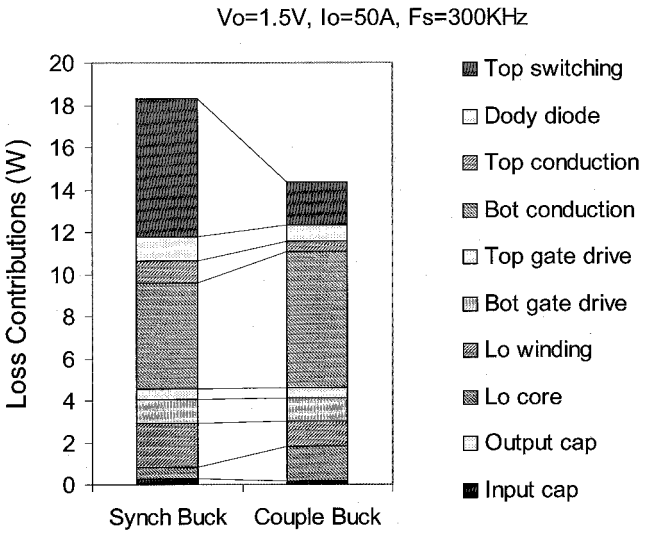

Fig. 21. Loss contributions for a four-phase coupled buck VRM and a four-phase buck VRM.

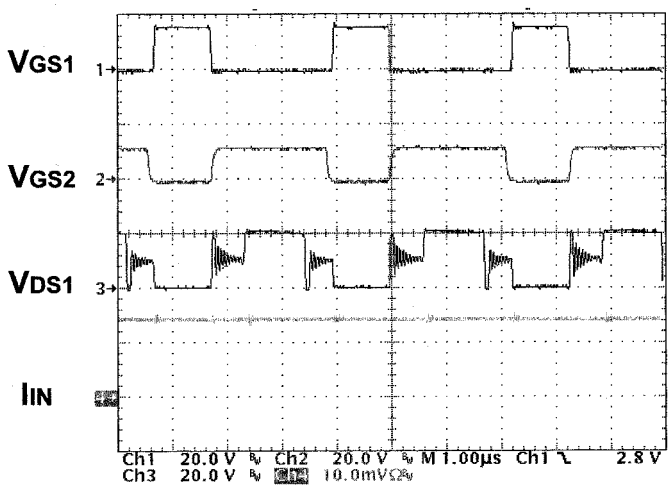

Fig. 22. Measured waveforms with a smooth input current in improved multiphase coupled-buck VRM.

Fig. 22 shows the measured waveforms at full load. The input current is ripple-free as shown in the bottom line, which proves the existence of built-in filters in the proposed multiphase coupled-buck converter.

VII. Conclusion

The influence of duty cycle on the performance of the multiphase buck converter has been studied. With a very small duty cycle, the benefit of the multiphase buck converter as far as using a small inductance to improve the transient response, is compromised due to poor ripple cancellation. The efficiency of multiphase buck converter also suffers from a very small duty cycle, mainly due to increased switching loss in the control MOSFETs.

In order to improve the efficiency without comprising the transient response, alternative topologies with extended duty cycles have been explored. One of the simplest topologies is multiphase tapped-inductor buck converter. However it suffers from the voltage spike problem caused by leakage inductance. This paper has proposed an improved topology named the multiphase

coupled-buck converter, which enables the use of a large duty cycle with recovered leakage energy and clamped MOSFET voltages. Both analysis and experiment have shown that the multiphase coupled-buck converter can have a much better efficiency than the multiphase buck converter with the same transient response.

The input filter has been further integrated in the proposed circuit to reduce the number of components. The improved multiphase coupled-buck converter features smooth input and output currents due to the existence of built-in filters.

REFERENCES

[1] Intel Corporation, *Proc. Intel Technol. Symp.*, Seattle, WA, Sept. 2001.

[2] X. Zhou, P. Xu, and F. C. Lee, "A high power density, high frequency and fast transient voltage regulator module with a novel current sharing and current sharing technique," in *Proc. IEEE APEC Conf.*, 1999, pp. 289–294.

[3] X. Zhou, P. Wong, P. Xu, F. C. Lee, and A. Q. Huang, "Investigation of candidate VRM topologies for future microprocessors," *IEEE Trans. Power Electron.*, pp. 1172–1182, Nov. 2000.

[4] P. Xu, X. Zhou, P. Wong, K. Yao, and F. C. Lee, "Design and performance evaluation of multi-channel interleaving quasisquare-wave buck voltage regulator module," in *Proc. HFPC'00 Conf.*, 2000, pp. 82–88.

[5] Y. Panov and M. M. Jovanovic, "Design consideration for 12-V/1.5-V, 50-A voltage regulator modules," *IEEE Trans. Power Electron.*, pp. 776–783, Nov. 2001.

[6] H. Matsuo and K. Harada, "The cascade connection of switching regulators," *IEEE Trans. Ind. Applicat.*, vol. IA-3, Mar./Apr. 1976.

[7] M. Rico, J. Uceda, J. Sebastian, and F. Aldana, "Static and dynamic modeling of tapped-inductor DC-to-DC converter," in *Proc. IEEE PESC'87 Conf.*, 1987, pp. 281–288.

[8] R. D. Middlebrook, "Transformerless DC-to-DC converters with large conversion ratio," in *Proc. IEEE INTELEC'84 Conf.*, 1984, pp. 455–460.

[9] D. Maksimovic and S. Cuk, "Switching converters with wide DC conversion range," *IEEE Trans. Power Electron.*, pp. 151–157, Jan. 1991.

[10] J. Wei, P. Xu, F. C. Lee, and M. Ye, "Static and dynamic modeling of the active clamp coupled-buck converter," in *Proc. IEEE PESC'01 Conf.*, 2001, pp. 260–265.

[11] E. Herbert, "Analysis of the near zero input current ripple condition in a symmetrical push–pull power converter," in *Proc. HFPC'89 Conf.*, 1989, pp. 357–371.

[12] C. Leu and J. Hwang, "A built-in input filter forward converter," in *Proc. IEEE PESC'94 Conf.*, 1994, pp. 917–921.

[13] R. Lai, K. D. T. Ngo, and J. K. Watson, "Steady-state analysis of the symmetrical push–pull power converter employing a matrix transformer," *IEEE Trans. Power Electron.*, pp. 44–52, Jan. 1992.

Peng Xu (S'00–M'02) received the B.S. and M.S. degrees in electrical engineering from Zhejiang University, Hangzhou, China, in 1994 and 1997, respectively, and the Ph.D. degree in electrical engineering from Center for Power Electronics Systems (CPES), Virginia Polytechnic Institute and State University, Blacksburg, VA, in 2002.

He has been a Senior Member of Research Staff, Philips Research—USA, Briarcliff Manor, NY, since January 2002. His research interests include low voltage power conversion, distributed power systems, power factor correction techniques, high-frequency magnetics and device characterization, and converter modeling and control.

Jia Wei received the B.S. degree in electrical engineering from Nanjing University of Aeronautics and Astronautics, Nanjing, China, in 1997, and the M.S. degree in electrical engineering from Center for Power Electronics Systems (CPES), Virginia Polytechnic Institute and State University, Blacksburg, VA, in 2002, where he is currently pursuing the Ph.D. degree in electrical engineering.

His research interests include distributed power systems, power factor correction techniques, low-voltage power supplies, modeling, and control.

Fred C. Lee (S'72–M'74–SM'87–F'90) received the B.S. degree in electrical engineering from the National Cheng Kung University, Taiwan, R.O.C., in 1968 and the M.S. and Ph.D. degrees in electrical engineering from Duke University, Durham, NC, in 1971 and 1974, respectively.

He is a University Distinguished Professor with Virginia Polytechnic Institute and State University (Virginia Tech), Blacksburg, and prior to that he was the Lewis A. Hester Chair of Engineering at Virginia Tech. He directs the Center for Power Electronics Systems (CPES), a National Science Foundation engineering research center whose participants include five universities and over 100 corporations. In addition to Virginia Tech, participating CPES universities are the University of Wisconsin-Madison, Rensselaer Polytechnic Institute, North Carolina A&T State University, and the University of Puerto Rico-Mayaguez. He is also the Founder and Director of the Virginia Power Electronics Center (VPEC), one of the largest university-based power electronics research centers in the country. VPECs Industry-University Partnership Program provides an effective mechanism for technology transfer, and an opportunity for industries to profit from VPECs research results. VPECs programs have been able to attract world-renowned faculty and visiting professors to Virginia Tech who, in turn, attract an excellent cadre of undergraduate and graduate students. Total sponsored research funding secured by him over the last 20 years exceeds $35 million. His research interests include high-frequency power conversion, distributed power systems, space power systems, power factor correction techniques, electronics packaging, high-frequency magnetics, device characterization, and modeling and control of converters. He holds 19 U.S. patents, and has published over 120 journal articles in refereed journals and more than 300 technical papers in conference proceedings.

Dr. Lee received the Society of Automotive Engineering's Ralph R. Teeter Education Award (1985), Virginia Tech's Alumni Award for Research Excellence (1990), and its College of Engineering Dean's Award for Excellence in Research (1997), in 1989, the William E. Newell Power Electronics Award, the highest award presented by the IEEE Power Electronics Society for outstanding achievement in the power electronics discipline, the Power Conversion and Intelligent Motion Award for Leadership in Power Electronics Education (1990), the Arthur E. Fury Award for Leadership and Innovation in Advancing Power Electronic Systems Technology (1998), the IEEE Millennium Medal, and honorary professorships from Shanghai University of Technology, Shanghai Railroad and Technology Institute, Nanjing Aeronautical Institute, Zhejiang University, and Tsinghua University. He is an active member in the professional community of power electronics engineers. He chaired the 1995 International Conference on Power Electronics and Drives Systems, which took place in Singapore, and co-chaired the 1994 International Power Electronics and Motion Control Conference, held in Beijing. During 1993-1994, he served as President of the IEEE Power Electronics Society and, before that, as Program Chair and then Conference Chair of IEEE-sponsored power electronics specialist conferences.